

## <sup>19</sup>F NMR Analysis of the Antimicrobial Peptide PGLa Bound to Native Cell Membranes from Bacterial Protoplasts and Human Erythrocytes

Marco Ieronimo,<sup>†</sup> Sergii Afonin,<sup>‡</sup> Katja Koch,<sup>†</sup> Marina Berditsch,<sup>†</sup> Parvesh Wadhvani,<sup>‡</sup> and Anne S. Ulrich<sup>\*,†,‡</sup>

*Institute of Organic Chemistry and DFG-Center for Functional Nanostructures, Karlsruhe Institute of Technology, Fritz-Haber-Weg 6, 76131 Karlsruhe, Germany, and Institute of Biological Interfaces (IBG-2), Karlsruhe Institute of Technology, P.O. Box 3640, 76021 Karlsruhe, Germany*

Received February 24, 2010; E-mail: anne.ulrich@kit.edu

In-cell NMR is highly informative as it can reveal structures, interactions, and dynamic behavior of soluble biomolecules in their genuinely natural environment.<sup>1–3</sup> Toward the same goal,<sup>4–6</sup> we demonstrate here that it is possible to analyze a membrane-active peptide bound to native biomembranes. Membrane-bound peptides and proteins are usually studied in model systems such as detergent micelles or in bilayers composed of synthetic lipids or lipid extracts. The only exception is bacteriorhodopsin in the purple membrane of *Halobacterium salinarium*,<sup>7–11</sup> besides some bound ligands or prosthetic groups, e.g., in rhodopsin, GalP, or AchR.<sup>12–17</sup> The effect of antimicrobial peptides on the membranes of living bacteria has been investigated by observing the phospholipids with <sup>31</sup>P NMR<sup>18</sup> because direct observation of peptides and proteins themselves in native biomembranes is hampered by the low sensitivity and natural abundance background of conventional <sup>2</sup>H, <sup>13</sup>C, or <sup>15</sup>N labels. Here, we demonstrate that <sup>19</sup>F NMR of a selectively labeled peptide can overcome both limitations.<sup>19–22</sup>

The antibiotic PGLa (GMASKAGAIAGKIAKVALKAL-NH<sub>2</sub>)<sup>23</sup> from *Xenopus laevis* was chosen as a case study, as it is available with selective 4-CF<sub>3</sub>-phenylglycine (CF<sub>3</sub>-Phg) <sup>19</sup>F labels by which it has been thoroughly characterized in model lipid bilayers.<sup>24–26</sup> The amphiphilic  $\alpha$ -helix was found to undergo a stepwise change in its membrane alignment from a surface-bound S-state, via an obliquely tilted T-state, to an inserted I-state that presumably represents an oligomeric transmembrane pore.<sup>27–29</sup> Its antimicrobial function is attributed to selective permeabilization of bacterial membranes,<sup>30</sup> while of course the cells of the host organism have to remain unharmed. To observe and compare PGLa in prokaryotic and eukaryotic cell membranes, we isolated native membranes from the Gram-positive bacterium *Micrococcus luteus* and from human erythrocytes. These preparations were optimized to serve as NMR samples, both as vesicular dispersions and by macroscopically aligning the membranes on glass plates.<sup>31</sup>

Solid-state <sup>31</sup>P NMR was used to monitor the purification of the membrane samples, as the lineshape of the native phospholipids is characteristic of their purity, lamellar state, and degree of alignment.<sup>32–35</sup> All <sup>31</sup>P-containing components, such as intracellular (oligo)nucleotides, had to be removed first. Purification by osmotic lysis and repeated washing/sedimentation cycles was readily achieved with erythrocytes but turned out to be much harder for bacterial protoplasts. For example, in our initial attempt to study *Bacillus subtilis*, the presence of extracellular teichoic acids produced a pronounced isotropic <sup>31</sup>P NMR signal (Supporting Information (SI), Figure S1). This signal cannot be discriminated from the typical signs of membrane disintegration like small vesicles or cubic phases. Therefore, *M. luteus* was chosen instead as a more

suitable Gram-positive organism lacking such membrane-anchored, phosphate-bridged polymers. The resulting <sup>31</sup>P NMR spectra of the native bacterial and erythrocyte membranes are illustrated in Figure 1 and compared with model lipid bilayers composed of dimyristoylphosphatidylcholine (DMPC). The powder lineshapes of all vesicular dispersion samples are characteristic of lamellar bilayers in the liquid crystalline state. The oriented samples show a narrow lipid signal, which is scaled by the expected factor of  $-1/2$  upon flipping the sample by 90° in the static magnetic field.<sup>24</sup> Only a slight isotropic contribution remains in the native membranes. The high quality of lipid alignment in these samples is remarkable and could be achieved by allowing the suspensions to sediment and dry on small glass plates under 96% humidity (SI). The broader mosaic spread in the *M. luteus* sample may be attributed to the fact that these membranes contain only about 28% total lipid by weight,<sup>36</sup> whereas erythrocyte ghosts contain up to 44%.<sup>37</sup>

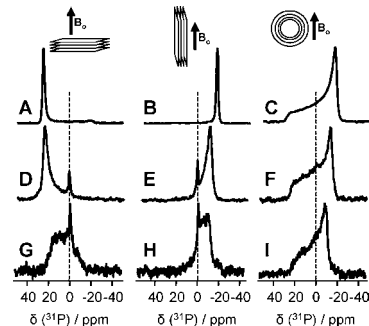


**Figure 1.** Solid-state <sup>31</sup>P NMR spectra of DMPC bilayers (A–C), erythrocyte ghosts (D–F), and *M. luteus* protoplast membranes (G–I). In oriented samples the membranes are deposited on glass supports, which are aligned with their normal either parallel (0°, A,D,G) or perpendicular (90°, B,E,H) to the static magnetic field direction. Non-oriented samples (C,F,I) exhibit a powder lineshape. The isotropic frequency is marked by a dotted line. All spectra were acquired at 308 K.

With suitable erythrocyte and protoplast membranes successfully prepared, <sup>19</sup>F NMR can now be used to examine the antimicrobial peptide PGLa in these NMR samples. Two different molar peptide–lipid ratios (P/L) of 1:300 and 1:40 were prepared by first quantifying the total phosphorus in the membrane suspension and then adding the necessary amount of peptide. The <sup>19</sup>F-labeled PGLa was incubated with the suspensions and co-sedimented by centrifugation (see SI for the sample preparation). The absence of any <sup>19</sup>F NMR signal in the supernatant confirmed its complete binding to the membranes.

When a peptide is labeled with a single CF<sub>3</sub>-Phg side chain and reconstituted in oriented membranes, the chemical shift anisotropy and dipolar splitting of the CF<sub>3</sub>-group yield a local orientational

<sup>†</sup> Institut für Organische Chemie, KIT.

<sup>‡</sup> Institut für Biologische Grenzflächen, KIT.

constraint for the labeled segment that is rigidly attached to the peptide backbone.<sup>19,20</sup> By combining several such constraints, PGLa has been previously characterized in terms of its  $\alpha$ -helical conformation, its membrane alignment, and its dynamic behavior in model lipid bilayers.<sup>24,25,29</sup> Those structural results had been independently verified by  $^2\text{H}$  NMR using entirely nonperturbing labels.<sup>26–28,38</sup> A set of reliable  $^{19}\text{F}$  NMR reference spectra is thus available for four different labeled PGLa analogues in DMPC/DMPG (3/1).<sup>29</sup> Each of these data sets covers the three distinct helix alignments in the S-, T-, and I-states (SI, Figure S2). On the basis of these data, we selected the  $\text{CF}_3$ -Phg label at position Ile13 to yield a unique fingerprint signal, by which the expected predominant S-state of the helical peptide can be readily identified. The characteristic feature of the oriented  $^{19}\text{F}$  NMR spectrum ( $0^\circ$  sample tilt) is a triplet with a dipolar splitting of about +6 kHz downfield from the isotropic frequency, as can be seen in Figure 2A. This signal appears in a convenient region of the spectrum that is not obscured by peaks from the powder pattern, which arises from non-oriented immobile peptides (with a splitting of about  $-7.5$  kHz upfield, marked with an asterisk in Figure 2). It can thus be stated: if the unique +6 kHz fingerprint splitting is observed in the spectrum of a macroscopically oriented sample, then PGLa must be bound to these membranes as a surface-aligned helix in the S-state.

Inspection of the data in Figure 2 demonstrates that, indeed, a selectively labeled peptide can be detected by  $^{19}\text{F}$  NMR in native membranes, even at a low concentration down to P/L = 1:300. For these simple  $^1\text{H}$ -decoupled 1D experiments at 470 MHz, the typical amount of PGLa was 0.1–0.5 mg in oriented erythrocyte ghosts, and the total dry weight of membrane material was about 17 mg, compared to 0.16 mg of PGLa in oriented DMPC/DMPG at P/L = 1:300. NMR measuring times were 12–36 h for the oriented ghosts at P/L = 1:300 (Figure 2C), 3–5 h for 1:40 (Figure 2E), and  $\sim 20$  h for the non-oriented preparations (Figure 2D,F), compared to 12–14 h for PGLa in oriented DMPC/DMPG at 1:300 (data not shown). These experimental conditions highlight the exquisite sensitivity of  $^{19}\text{F}$  labels, notably with no background subtraction necessary nor any referencing required.<sup>39</sup>

Next, some genuine structural information can be derived on PGLa bound to the native biomembranes. As outlined above, the characteristic S-state fingerprint signal with a +6 kHz dipolar splitting is clearly seen in the erythrocyte samples at P/L = 1:300 at 308 K (Figure 2C), and also for 1:40 at an elevated temperature of 343 K (Figure 2E, upper trace). Note that in the 1:2:1 triplet signals of oriented  $\text{CF}_3$ -Phg labels, the outermost component (relative to the isotropic position) is broadened due to mosaic spread and  $T_2$  relaxation;<sup>24</sup> hence, it is readily obscured as in the present examples. In contrast, the innermost triplet component is sharp and intense, but it happens to lie almost at the isotropic frequency and will overlap there with the innermost (sharp) peak from any powder contribution. Therefore, the decisive sign of a typical  $\text{CF}_3$ -group triplet is the presence of its central component, shifted up or down from the isotropic frequency by the appropriate splitting.

The presence of the fingerprint signal demonstrates that a fraction of PGLa is bound to native ghost membranes as a surface-aligned  $\alpha$ -helix. Upon changing the sample tilt to  $90^\circ$ , this signal gets flipped by a factor of  $-1/2$  upfield (SI, Figure S3). The same effect is seen in the non-oriented samples, which exhibit a narrow powder pattern with a splitting of +3 kHz (Figure 2B,D,F). Such spectral behavior is characteristic of in-plane motional averaging of the peptide molecules, suggesting that indeed a significant fraction of PGLa is membrane-bound in the S-state and undergoes rapid in-plane diffusion on a millisecond time scale.

Even though the oriented bacterial protoplasts suffer from considerable mosaic spread (see Figure 1), a distinct +6 kHz shoulder appears in the relevant spectral region (Figure 2G) and obeys the same changes with sample geometry (Figure 2H).

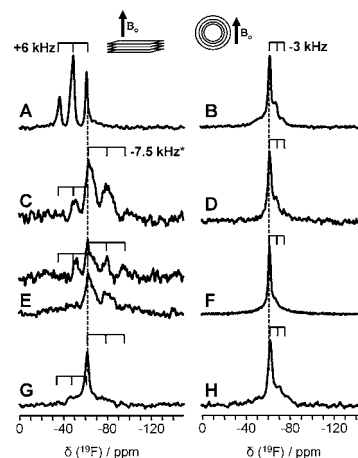


**Figure 2.** Solid-state  $^{19}\text{F}$  NMR spectra of the antimicrobial peptide PGLa (labeled with  $\text{CF}_3$ -Phg at position Ile13) in DMPC/DMPG bilayers (A,B; see SI for full data set), in erythrocyte ghosts (C–F), and in *M. luteus* protoplast membranes (G,H). The P/L is either 1:300 (C,D) or 1:40 (E–H). All spectra were acquired at 308 K, except for the upper trace in panel E at 343 K. The oriented membranes at  $0^\circ$  sample tilt (left panels) were prepared at 96% relative humidity, and the non-oriented samples (right panels) contain excess water. The dipolar splitting of +6.0 kHz (marked, see text) is a fingerprint for the surface-bound S-state of the  $\alpha$ -helical peptide, as known from studies in model membranes (A,B and SI, Figure S2). The isotropic frequency is indicated with a dotted line, and peaks from the powder pattern of immobilized peptides are marked by asterisks.

Besides the well-aligned S-state of PGLa bound to the bilayer surface, we may also try to discriminate other states of the peptide in the native membrane preparations. Their respective proportions can be estimated from the corresponding intensities of the single-pulse  $^{19}\text{F}$  NMR spectra in Figure 2. Notable is the occurrence of an immobilized fraction of non-oriented PGLa, which gives rise to a Pake triplet with a  $-7.5$  kHz splitting. It actually dominates the oriented erythrocyte spectra at 308 K (Figure 2C,E), but its intensity relative to the fingerprint signal gets reduced with increasing temperature (see upper trace in Figure 2E and SI, Figure 4S). We attribute the immobilized peptide population to PGLa molecules that are non-specifically bound to the anionic erythrocyte glycocalyx under the limited hydration conditions of these oriented samples (96% relative humidity, and see below).

The selected  $\text{CF}_3$ -Phg label is ideally suited to discriminate the S-state (+6 kHz) from the T- and I-states ( $-2.5$  and  $-4$  kHz, respectively, see SI, Figure 2S). Neither of the latter alignment states is expected to dominate the behavior of PGLa under the conditions studied here; hence, it does not matter that their smaller splittings may not be so readily discernible. Nevertheless, the isotropic frequency region deserves attention, since an isotropic signal is indicative of unbound peptides that are free to undergo complete motional averaging on the millisecond time scale.<sup>27</sup> This effect is best visualized in the non-oriented samples of Figure 2, which contain excess water and therefore do not exhibit any signals from immobilized peptides. As noted above, the partially averaged  $^{19}\text{F}$  NMR powder patterns with a +3 kHz splitting fully support the S-state alignment of PGLa. These lineshapes account for virtually the total spectral intensity of the differentially broadened Pake triplet in the anionic DMPC/DMPG bilayers (Figure 2B), the erythrocyte sample at P/L = 1:300 (Figure 2D), and the protoplast membranes

at 1:40 (Figure 2H). On the other hand, in the non-oriented erythrocyte membranes at P/L = 1:40, there remains a considerable amount of unbound peptide, as the isotropic signal contributes about half the total intensity (Figure 2F). We thus conclude that, in the compacted suspension samples, which are prepared by high-speed centrifugation, the protoplast membranes are able to bind about 10-fold more PGLa than the erythrocyte ghosts (i.e., 1:300 looks like 1:40). This different affinity agrees well with the known selectivity of antimicrobial peptides toward bacteria. The binding of cationic peptides to prokaryotic membranes is driven by electrostatic interactions with the anionic lipids that are abundant on the bacterial surface, whereas eukaryotic cells possess mainly zwitterionic lipids in their outer monolayer.<sup>40–42</sup> Also the presence of cholesterol, which is abundant in erythrocytes but absent in bacteria, is known to protect membranes from insertion of antimicrobial peptides.<sup>43</sup>

In summary, we demonstrate that <sup>19</sup>F-labeled peptides can be detected by NMR and can be structurally characterized when bound to native membranes from eukaryotic and prokaryotic cells. A single, carefully chosen CF<sub>3</sub>-Phg label on the antimicrobial peptide PGLa was sufficient to prove that this amphiphilic  $\alpha$ -helix is aligned flat on the lipid bilayer surface, both in erythrocyte ghosts and in *M. luteus* protoplasts. The membrane preparations were optimized for oriented NMR analysis by examining the <sup>31</sup>P signals of the phospholipids (as *M. luteus* lacks other interfering phosphate-containing cell envelope components).

Oriented samples are essential for an unbiased <sup>19</sup>F NMR analysis, but due to their limited hydration it seems that a certain fraction of PGLa was trapped in a non-aligned and immobilized state. Physiologically more relevant are the non-oriented samples containing excess water, where PGLa was always seen to be well-aligned in the S-state. Only at high P/L (1:40), some PGLa remained unbound in erythrocytes. The bacterial membranes, on the other hand, were able to accommodate all of the peptide at this concentration, which corresponds roughly to the critical threshold where antimicrobial action is known to induce membrane disruption.<sup>42,44,45</sup> As we identified the S-state to be the predominant helix alignment under equilibrium conditions, it is likely that pore formation in living cells is a short-lived event, transiently induced by the lateral pressure of peptides accumulating in the outer monolayer.<sup>46</sup> In synthetic lipid membranes it has been possible to trap the inserted I-state only under special conditions, such as in the presence of its synergistic partner magainin 2<sup>27</sup> or in the lipid gel phase.<sup>29</sup>

**Supporting Information Available:** Experimental procedures and supporting Figures S1–S4. This material is available free of charge via the Internet at <http://pubs.acs.org>.

## References

- Reckel, S.; Hänsel, R.; Löhr, F.; Dötsch, V. *Prog. NMR Spectrosc.* **2007**, *51*, 91–101.
- Selenko, P.; Wagner, G. *J. Struct. Biol.* **2007**, *158*, 244–253.
- Sakakibara, D.; Sasaki, A.; Ikeya, T.; Hamatsu, J.; Hanashima, T.; Mishima, M.; Yoshimasu, M.; Hayashi, N.; Mikawa, T.; Wälchli, M.; Smith, B. O.; Shirakawa, M.; Güntert, P.; Ito, Y. *Nature* **2009**, *458*, 102–105.
- Curtis-Fisk, J.; Spencer, R. M.; Weliky, D. P. *J. Am. Chem. Soc.* **2008**, *130*, 12568–12569.
- Fowler, D. J.; Weis, R. M.; Thompson, L. K. *Biochemistry* **2010**, *49*, 1425–1434.
- Kim, S. J.; Cegelski, L.; Preobrazhenskaya, M.; Schaefer, J. *Biochemistry* **2006**, *45*, 5235–5250.
- Ulrich, A. S.; Wallat, I.; Heyn, M. P.; Watts, A. *Nat. Struct. Biol.* **1995**, *2*, 190–192.
- Kamihira, M.; Vosegaard, T.; Mason, A. J.; Straus, S. K.; Nielsen, N. C.; Watts, A. *J. Struct. Biol.* **2005**, *149*, 7–16.
- Brown, M. F.; Heyn, M. P.; Job, C.; Kim, S.; Moltke, S.; Nakanishi, K.; Nevzorov, A. A.; Struts, A. V.; Salgado, G. F.; Wallat, I. *Biochim. Biophys. Acta* **2007**, *1768*, 2979–3000.
- Lopez, J. J.; Mason, A. J.; Kaiser, C.; Glaubitz, C. *J. Biomol. NMR* **2007**, *37*, 97–111.
- Varga, K.; Aslimovska, L.; Watts, A. *J. Biomol. NMR* **2008**, *41*, 1–4.
- Spooner, P. J.; Rutherford, N. G.; Watts, A.; Henderson, P. J. *Proc. Natl. Acad. Sci. U.S.A.* **1994**, *91*, 3877–3881.
- Williamson, P. T.; Watts, J. A.; Addona, G. H.; Miller, K. W.; Watts, A. *Proc. Natl. Acad. Sci. U.S.A.* **2001**, *98*, 2346–2351.
- Spooner, P. J.; Sharples, J. M.; Verhoeven, M. A.; Lugtenburg, J.; Glaubitz, C.; Watts, A. *Biochemistry* **2002**, *41*, 7549–7555.
- Patching, S. G.; Psakis, G.; Baldwin, S. A.; Baldwin, J.; Henderson, P. J.; Middleton, D. A. *Mol. Membr. Biol.* **2008**, *25*, 474–484.
- Krabben, L.; van Rossum, B. J.; Jehle, S.; Bocharov, E.; Lyukmanova, E. N.; Schulga, A. A.; Arseniev, A.; Hucho, F.; Oschkinat, H. *J. Mol. Biol.* **2009**, *390*, 662–671.
- Williamson, P. T.; Verhoeven, A.; Miller, K. W.; Meier, B. H.; Watts, A. *Proc. Natl. Acad. Sci. U.S.A.* **2007**, *104*, 18031–18036.
- Chia, B. C. S.; Lam, Y.-H.; Dyall-Smith, M.; Separovic, F.; Bowie, J. H. *Leit. Pept. Sci.* **2000**, *7*, 151–156.
- Ulrich, A. S. *Prog. NMR Spectrosc.* **2005**, *46*, 1–21.
- Ulrich, A. S. In *Modern Magnetic Resonance*; Webb, G. A., Ed.; Springer: Berlin, 2007; Part I, pp 257–263.
- Chekmenov, E. Y.; Chow, S. K.; Tofan, D.; Weitekamp, D. P.; Ross, B. D.; Bhattacharya, P. *J. Phys. Chem. B* **2008**, *112*, 6285–6287.
- Grage, S. L.; Afonin, S.; Ulrich, A. S. *Methods Mol. Biol.* **2010**, *618*, 183–207.
- Soravia, E.; Martini, G.; Zasloff, M. *FEBS Lett.* **1988**, *228*, 337–340.
- Glaser, R. W.; Sachse, C.; Dürr, U. H. N.; Wadhvani, P.; Ulrich, A. S. *J. Magn. Reson.* **2004**, *168*, 153–163.
- Glaser, R. W.; Sachse, C.; Dürr, U. H. N.; Wadhvani, P.; Afonin, S.; Strandberg, E.; Ulrich, A. S. *Biophys. J.* **2005**, *88*, 3392–3397.
- Strandberg, E.; Wadhvani, P.; Tremouilhac, P.; Dürr, U. H. N.; Ulrich, A. S. *Biophys. J.* **2006**, *90*, 1676–1686.
- Tremouilhac, P.; Strandberg, E.; Wadhvani, P.; Ulrich, A. S. *Biochim. Biophys. Acta* **2006**, *1758*, 1330–1342.
- Tremouilhac, P.; Strandberg, E.; Wadhvani, P.; Ulrich, A. S. *J. Biol. Chem.* **2006**, *281*, 32089–32094.
- Afonin, S.; Grage, S. L.; Ieronimo, M.; Wadhvani, P.; Ulrich, A. S. *J. Am. Chem. Soc.* **2008**, *130*, 16512–16511.
- Hara, T.; Mitani, Y.; Tanaka, K.; Uematsu, N.; Takakura, A.; Tachi, T.; Kodama, H.; Kondo, M.; Mori, H.; Otaka, A.; Nobutaka, F.; Matsuzaki, K. *Biochemistry* **2001**, *40*, 12395–12399.
- Gröbner, G.; Taylor, A.; Williamson, P. T.; Choi, G.; Glaubitz, C.; Watts, J. A.; de Grip, W. J.; Watts, A. *Anal. Biochem.* **1997**, *254*, 132–138.
- Auger, M. *Curr. Issues Mol. Biol.* **2000**, *2*, 119–124.
- Drechsler, A.; Separovic, F. *IUBMB Life* **2003**, *55*, 515–523.
- Moreau, C.; Le Floch, M.; Segalen, J.; Leray, G.; Metzinger, L.; de Certaines, J. D.; Le Rumeur, E. *FEBS Lett.* **1999**, *461*, 258–262.
- Yeagle, P. L. *Biophys. J.* **1982**, *37*, 227–239.
- Gilby, A. R.; Few, A. V.; McQuillen, K. *Biochim. Biophys. Acta* **1958**, *29*, 21–29.
- Rosenberg, S. A.; Guidotti, G. *J. Biol. Chem.* **1968**, *243*, 1985–1992.
- Strandberg, E.; Tremouilhac, P.; Wadhvani, P.; Ulrich, A. S. *Biochim. Biophys. Acta* **2009**, *1788*, 1667–1679.
- Glaser, R. W.; Ulrich, A. S. *J. Magn. Reson.* **2003**, *164*, 104–114.
- Yeaman, M. R.; Yount, N. Y. *Pharmacol. Rev.* **2003**, *55*, 27–55.
- Quinn, P. J. *Subcell. Biochem.* **2002**, *36*, 39–60.
- Matsuzaki, K. *Biochim. Biophys. Acta* **2009**, *1788*, 1687–1692.
- Matsuzaki, K.; Sugishita, K.; Fujii, N.; Miyajima, K. *Biochemistry* **1995**, *34*, 3423–3429.
- Blazyk, J.; Wiegand, R.; Klein, J.; Hammer, J.; Epanand, R. M.; Epanand, R. F.; Maloy, W. L.; Kari, U. P. *J. Biol. Chem.* **2001**, *276*, 27899–27906.
- Melo, M. N.; Ferre, R.; Castanho, M. A. *Nat. Rev. Microbiol.* **2009**, *7*, 245–250.
- Matsuzaki, K.; Murase, O.; Fujii, N.; Miyajima, K. *Biochemistry* **1995**, *34*, 6521–65263.

JA101608Z